

The Angstrom Project survey of M31 bulge microlensing

Eamonn Kerins*

Jodrell Bank Centre for Astrophysics, The University of Manchester, UK

E-mail: Eamonn.Kerins@manchester.ac.uk

on behalf of the Angstrom Project team

The Andromeda Galaxy Stellar Robotic Microlensing (Angstrom) Project[†] is surveying the bulge of the Andromeda Galaxy (M31) for microlensing events, transients and variable stars. Its science goals are: i) constraining the 3D structure of the M31 bulge using the spatial distribution of microlensing events and variable stars; ii) measuring the abundance of low-mass stars within the M31 bulge; iii) compiling a catalogue of short-timescale variables and transients; iv) real-time flagging and follow-up of ongoing microlensing events. Here I overview the exciting potential offered by M31 stellar microlensing, from extragalactic structure studies through to extra-galactic planet detection. I shall describe the Angstrom Project telescope network and real-time data reduction pipeline. The Angstrom Project is the first survey to attempt real-time microlensing discovery outside of the Milky Way; I present the milestones we have reached and the technical challenges we are facing.

The Manchester Microlensing Conference: The 12th International Conference and ANGLES Microlensing Workshop

January 21-25 2008

Manchester, UK

*On behalf of the Angstrom Project team

[†]<http://www.astro.livjm.ac.uk/angstrom/>

1. M31 microlensing: opportunities and challenges

Microlensing within the Milky Way is now a routinely detected phenomenon, with 3-4 new events detected every day during the bulge observing season. However it has been known for some time that microlensing can also be observed towards M31 [1, 2]. The original motivation for Milky Way and M31 microlensing surveys was the same: to detect or constrain the Macho dark matter hypothesis. This led to Milky Way surveys towards the Magellanic Clouds and wide-field surveys of the M31 disk. Today the most exciting microlensing discoveries are coming from the Milky Way bulge surveys monitoring stellar microlensing events. The ability to detect ongoing events in real-time has enabled high time resolution photometry of individual events, revealing deviations from standard microlensing profiles due to finite source effects, parallax effects or binary lens systems, sometimes including planetary lens companions. The large catalogue of events towards the bulge also holds great promise for galactic structure studies.

Just as for MACHO searches, the Andromeda Galaxy provides an attractive target for stellar microlensing studies [3]. It comprises a prominent bulge of which we have a largely unobstructed view. In one respect monitoring M31 bulge stars is much easier than monitoring the Milky Way bulge: the entire M31 bulge can be covered easily by a single telescope pointing. However, there are also substantial technical and theoretical limitations to M31 microlensing.

Theoretically speaking, there are significant limitations to the physics one can extract from M31 microlensing events. Firstly, whilst blending often affects Milky Way microlensing events it occurs at a relatively modest level and lightcurve fitting can often provide a reliable measure of the blending fraction and of the underlying Einstein radius crossing time, t_e , of the microlensing event. This is rarely possible with M31 microlensing. Detectable M31 microlensing events typically must have large magnifications to be seen against the background M31 surface brightness. In the high magnification limit the flux enhancement due to microlensing is described by:

$$\Delta F(t) = [A(t) - 1]F_s \simeq \frac{\Delta F(t_0)}{\sqrt{1 + 12 \left(\frac{t - t_0}{t_{1/2}}\right)^2}}, \quad (1.1)$$

where A is the event magnification at time t , F_s is the source flux in the absence of lensing, $t_{1/2}$ is the full-width at half-maximum timescale of the lightcurve, and t_0 is the epoch of maximum magnification. For a single passband the excess lightcurve depends only on 3 parameters $[t_0, t_{1/2}, \Delta F(t_0)]$ rather than the usual 4 parameters which describe the flux excess of the full non-degenerate Paczyński lightcurve. The result of this is that, in the absence of very high signal-to-noise ratio photometry, F_s and t_e cannot be determined uniquely from $t_{1/2} \simeq 2\sqrt{3}u_0t_e$ and $\Delta F(t_0) \simeq F_s/u_0$, where $u_0 \simeq A(t_0)^{-1}$ is the minimum lens-source impact distance in units of the Einstein radius. Individually, therefore, M31 microlensing events yield less information on source and lens parameters than their Milky Way counterparts.

A second limitation evident from Equation (1.1) is that the characteristic timescale over which an M31 event is detectable ($t_{1/2}$) can be much less than the underlying event timescale (t_e). For example, events within the M31 bulge typically require $u_0 \sim 0.03 - 0.1$ to be detectable against the background bulge light. In this case $t_{1/2}$ may be an order of magnitude smaller than t_e . Detailed semi-analytic calculations suggest that most M31 bulge events will be visible for between 1 – 10

days. To robustly detect and characterise events at the lower end of this timescale range requires telescopes sited at more than one location to give multiple observations per day.

A further limitation comes from finite source size considerations. For the source to undergo significant magnification the lens–source angular separation must be $\theta < \theta_e \propto M^{1/2}$, where θ_e is the angular Einstein radius and M is the lens mass. However, if $\theta < \theta_e \ll \theta_s$, where θ_s is the angular size of the source star, the magnification averaged over the source becomes negligible. There is therefore a minimum lens mass M_{\min} below which magnification effects are unobservable against typical sources. Since the line-of-sight distance between lens and source is similar for both Milky Way and M31 microlensing, the limiting mass simply scales as $M_{\lim} \propto d_l^2/u_0$, where d_l is the distance of the lens from the observer. Comparing typical Milky Way events ($d_l \sim 7$ kpc, $u_0 \sim 0.5$) with M31 events ($d_l \sim 780$ kpc, $u_0 \sim 0.1$) we see that the mass limit for M31 events is at least four orders of magnitude larger than for Milky Way events, with $M_{\lim}(\text{M31}) \sim 10^{-4} M_{\odot}$. However, finite source size limits are not all bad news for M31 microlensing. Whilst it is clear that they exclude using microlensing to detect Earth-like planets in M31, amazingly they do not exclude the detection of gas giant planets there (more on this later). Also, since finite source effects are more common for M31 events, it should be possible to study M31 stellar atmosphere profiles.

Lastly, M31 microlensing is intrinsically biased towards the detection of higher magnification events. Exotic microlensing systems, such as caustic-crossing binaries involving high magnification bursts, will therefore comprise a higher fraction of event samples and therefore cannot be safely ignored in optical depth measurements [4]. However, they also provide an opportunity to study the physics of the binary lens system itself and may, through finite source effects, allow the atmosphere of the source star to be probed. So, this can be equally seen as a positive benefit of M31 microlensing.

On the technical side up until now no M31 microlensing survey has been able to reduce its data in real time. The paucity of resolved stars in the M31 disk and bulge, together with the large surface brightness gradients within the bulge, makes difference imaging difficult to perform in a way which is sufficiently robust for an automated pipeline. The extreme levels of stellar crowding also mean that even variable objects approach the crowding limit within the M31 bulge [5]. This not only makes variable source identification difficult, it also means that lightcurves are contaminated by variations in nearby objects which have overlapping point spread functions. Lastly, the fact that M31 is 100 times further away than the Milky Way bulge means that we cannot expect the same level of photometric quality as is the case for Milky Way events. Despite these challenges the huge success of the Milky Way bulge surveys serves to inspire us to try to do similar science towards M31. This is the essential motivation driving the Angstrom Project.

2. The Angstrom Project

The Andromeda Galaxy Stellar Robotic Microlensing (Angstrom) Project is a collaboration involving astronomers based in the UK, Korea, USA and Uzbekistan. Angstrom operates a distributed network of 2m-class Northern hemisphere optical telescopes which monitors the M31 bulge several times per night during the M31 observing season, which runs from August through to February.

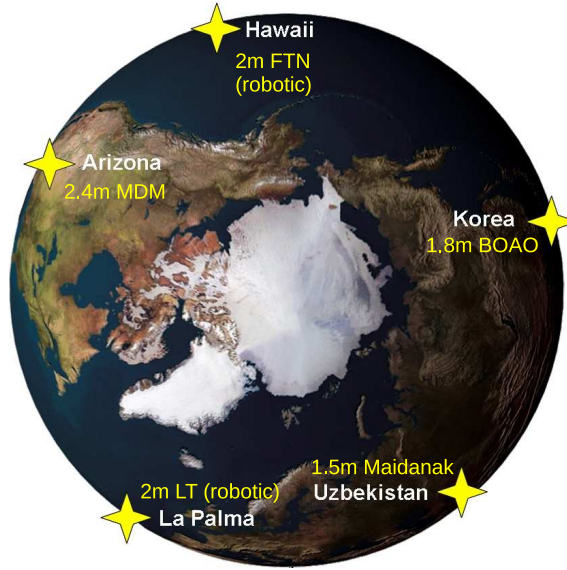


Figure 1: The geographical coverage of the Angstrom Project telescope network, permitting continuous observations of the M31 bulge.

Telescope	Field of view (arcmins)	Camera size (pixels)	Filter
2m LT, La Palma	4.6	2k×2k	Sloan <i>i</i>
2m FTN, Hawaii	4.6	2k×2k	Sloan <i>i</i>
1.5m Maidanak, Uzbekistan	18	4k×4k	Cousins <i>I</i>
1.8m BOAO, South Korea	11	2k×2k	Cousins <i>I</i>
2.4m MDM, Arizona	4.6	1k×1k	Cousins <i>I</i>

Table 1: The Angstrom Project telescopes and camera characteristics.

The Angstrom Project began taking data in Autumn 2004, initially using two telescopes: the 2m robotic Liverpool Telescope (LT) in the Canary Islands and the 1.8m at Bohyunsan Optical Astronomy Observatory (BOAO) in South Korea. Since 2004 the Angstrom Project telescope network has expanded to include three other 2m-class facilities: the 2.4m at MDM in Arizona, the 2m robotic Faulkes Telescope North (FTN) in Hawaii and the 1.5m at Maidanak Observatory in Uzbekistan. The use of multiple telescopes at well separated longitudes is necessary in order to detect and characterise variations as short as 1 day. Their geographical locations are shown in Figure 1. At any given time usually only two or three telescopes are available for observations. Currently the bulk of our data comes from the LT, FTN and the 1.5m at Maidanak, allowing continuous 24-hour coverage of the M31 bulge.

Observations are undertaken in Sloan *i* or Cousins *I* filters as these provide good discrimination against periodic variables such as Miras which tend to be most obvious in these bandpasses. The size of the field varies between the telescopes, from 4.6 arcmin for the robotic LT up to 18 arcmin for the 1.5m at Maidanak. However even the relatively small LT field is big enough to cover most

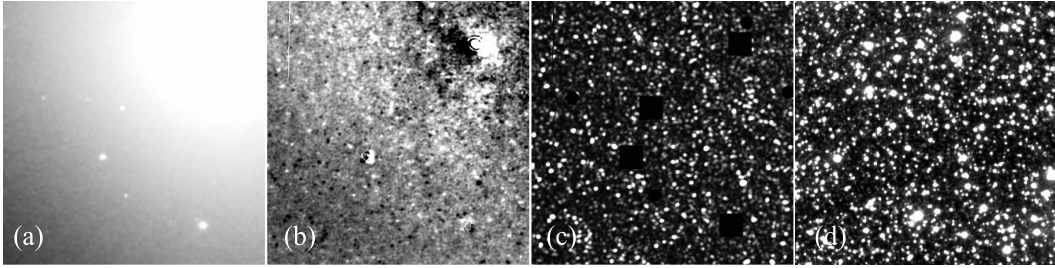


Figure 2: The Angstrom Data Analysis Pipeline. *From left to right:* (a) a 2 arcmin region of an LT *i*-band exposure. The core of the M31 bulge is at the top right; (b) the corresponding difference image showing black and white spots where objects have dimmed or brightened. Strong residuals are seen around the imperfectly subtracted core; (c) the significance map of variable sources, showing that variable objects near the M31 bulge approach the crowding limit; (d) an OGLE-III *I*-band image for comparison, where most of the objects on this image are not variable.

of the M31 bulge so only one pointing is necessary. The telescope and camera characteristics are summarised in Table 1. Typical exposures times are around 30 mins, comprising a stack of short exposures in order to minimise saturation of the core of the bulge.

3. Real-time detection towards M31

The two robotic telescopes (LT and FTN) operate without human intervention. When observations are taken they are automatically pre-processed and then made available for download usually within 10 minutes of observation. This allows data from these telescopes to be processed rapidly using an automated pipeline, and to this end we have developed the Angstrom Data Analysis Pipeline (ADAP) to take advantage of this. ADAP performs de-fringing and stacking of individual exposures before differencing the stack with a reference image. It then performs object detection on the difference images, produces PSF-fit photometry of the detected objects, matches detected objects with previously identified sources and then updates the photometry database with the new photometry. This procedure takes around two hours for each new image stack. Figure 2 shows images created at key intermediate steps of the processing.

Data from the non-robotic telescopes are processed offline but using essentially the same processing steps as for the ADAP processing of the robotic data. As and when the non-robotic data is processed it is added to the ADAP lightcurve photometry database. Additionally, we have also ingested into the ADAP four seasons of data from the POINT-AGAPE dark matter survey of M31 [6]. This data has been re-reduced by ourselves using the same difference image processing as used in the ADAP. The POINT-AGAPE data extends over about 60% of the image area of the LT/FTN fields and so increases the baseline coverage by an additional four years in these areas.

To exploit the real-time capability of ADAP we have developed the Angstrom Project Alert System (APAS) [5]. APAS interrogates the ADAP database for significant transient-like variations which may be interesting for follow-up. Because of the high crowding levels of variable objects it is often not possible to detect isolated transient signals within the lightcurves. For this reason the approach of APAS is to shortlist around ~ 50 of the most interesting variations (showing a burst

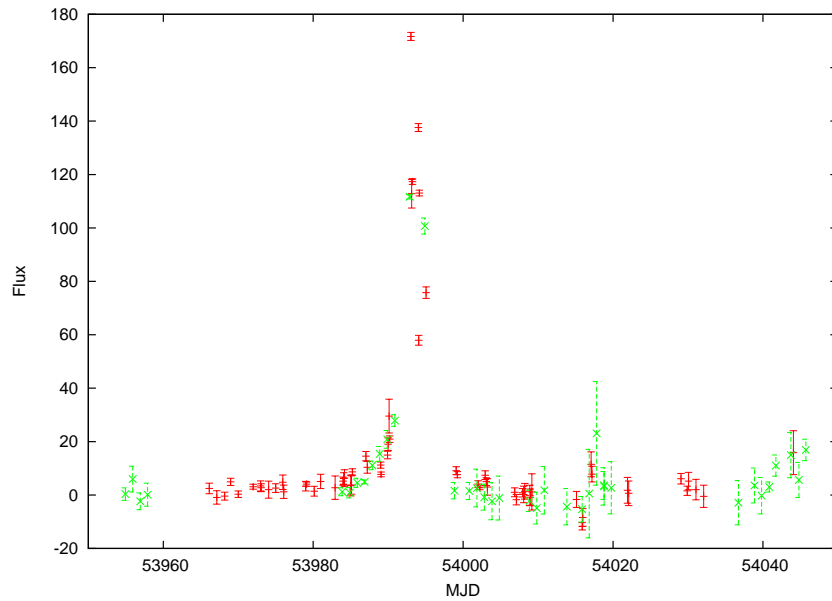


Figure 3: A short duration lightcurve consistent with microlensing with $t_{1/2} \simeq 2$ days. Red data is from LT (robotic), green is from Maidanak (non-robotic).

which is significantly above other activity around the baseline). The objects are flagged as alerts and their lightcurves are presented on a webpage for a human to make a decision on follow-up. To aid the decision APAS also catalogues all neighbouring variations within 3 arcsec of the flagged objects. For the robotic data this is the first point at which a human interacts with the data.

APAS was deployed in testing mode towards the end of the 2006/7 season and more systematically during the recent 2007/8 season. During the 2006/7 commissioning season APAS flagged a high signal-to-noise ratio lightcurve which is an excellent short microlensing candidate (Figure 3). During the 2007/8 season, we issued the first formal Angstrom alert on a Nova candidate [7]. Unfortunately the evolution of the lightcurve of this event subsequently revealed systematic errors with the pipeline photometry which has impacted significantly on our alert efficiency. The errors appear to be due to DIA object shifts induced by imperfect subtraction of the very steep bulge surface brightness gradient. A fix for this is currently being worked upon and we are hopeful that the alert efficiency will be much improved for the coming season. Our expectation for a fully-working alert system is that we should trigger on around half a dozen alerts per season.

4. Where we are and where we are going

Early results from the APAS indicates that real-time microlensing discovery is possible even towards external galaxies such as M31. However our pipeline is not yet fully robust and therefore is not yet operating at full efficiency. Between the end of the 2007/8 season (at the end of February 2008) and the start of the 2008/9 season (in August 2008) we will be working to fix the systematic photometry problems uncovered during the first full run of APAS.

Real-time M31 microlensing offers some very interesting possibilities for binary event detection and for finite-source size detection. Possibly the most exciting application is the detection of gas giant planets in M31. Microlensing is the only technique capable of detecting planets in another galaxy. Being able to probe even part of the planet discovery space towards another galaxy will help to understand to what extent planet formation is sensitive to stellar population characteristics. We have undertaken a theoretical study of the detectability of planets towards M31 [8]. Since M31 microlensing events are typically of high intrinsic magnification there is a very strong possibility that the source trajectory may cross the central caustic and therefore produce a detectable planetary signature. We have performed detailed simulations under different assumptions of alert strategy in order to assess the likelihood of being able to detect planets. The simulations indicate that finite source size effects preclude the possibility of detecting planets with masses much less than that of Saturn. However, we find that with 8m-class follow-up of an alerted event the planet detection efficiency can be as high as 40 – 60% for Jupiter mass planets.

Acknowledgments

This project is made possible by generous time allocations from the Science and Technology Facilities Council (STFC), the Time Allocation Committee at Liverpool JMU, and Rachel Street at Las Cumbres Observatory. I also wish to thank staff at Maidanak Observatory and the Bohyunsan Optical Astronomy Observatory for their help. I also wish to acknowledge financial support from the STFC.

References

- [1] Crotts, A., 1992, ApJ, 399, 43
- [2] Kerins, E. et al., 2001, MNRAS, 323, 13
- [3] Kerins, E. et al., 2006, MNRAS, 365, 1099
- [4] Kim, D. et al., 2007, ApJ, 666, 236
- [5] Darnley, M. et al., 2007, ApJ, 661, 45
- [6] Calchi Novati, S. et al., 2005, A&A, 443, 911
- [7] Darnley, M., Kerins, E., Newsam, A., 2007, The Astronomer's Telegram, 1192, 1
- [8] Chung, S.-J., 2006, ApJ, 650, 432